



ELSEVIER

Available online at [www.sciencedirect.com](http://www.sciencedirect.com)

ScienceDirect

journal homepage: [www.elsevier.com/locate/ijhe](http://www.elsevier.com/locate/ijhe)

## High-performance enzymatic biofuel cell based on three-dimensional graphene

Arman Amani Babadi <sup>a,\*</sup>, Wan Abd Al Qadr Imad Wan-Mohtar <sup>a,b</sup>,  
Jo-Shu Chang <sup>c,d</sup>, Zul Ilham <sup>b,e</sup>, Adi Ainurzaman Jamaludin <sup>b,e</sup>,  
Golnoush Zamiri <sup>f</sup>, Omid Akbarzadeh <sup>g</sup>, Wan Jefrey Basirun <sup>h</sup>

<sup>a</sup> Functional Omics and Bioprocess Development Laboratory, Institute of Biological Sciences, Faculty of Science, University of Malaya, 50603, Kuala Lumpur, Malaysia

<sup>b</sup> Bioresources and Bioprocessing Research Group, Institute of Biological Sciences, Faculty of Sciences, University of Malaya, 50603, Kuala Lumpur, Malaysia

<sup>c</sup> Department of Chemical Engineering, National Cheng Kung University, Tainan, Taiwan

<sup>d</sup> College of Engineering, Tunghai University, Taichung, Taiwan

<sup>e</sup> Environmental Science and Management Program, Institute of Biological Sciences, Faculty of Science, University of Malaya, 50603, Kuala Lumpur, Malaysia

<sup>f</sup> Centre of Advanced Materials, Mechanical Engineering, Faculty of Engineering, University of Malaya, 50603, Kuala Lumpur, Malaysia

<sup>g</sup> Nanotechnology & Catalysis Research Centre, University of Malaya, Kuala Lumpur, 50603, Malaysia

<sup>h</sup> Department of Chemistry, University of Malaya, Kuala Lumpur, 50603, Malaysia

### HIGHLIGHTS

- The performance of the enzymatic biofuelcell has enhanced.
- 3-dimensional graphene improve the electron transfer.
- 3-dimensional graphene decrease enzyme leaking.
- 3-dimensional graphene facilitate DET.
- Power density of 164  $\mu\text{W cm}^{-2}$  achieved.

### ARTICLE INFO

#### Article history:

Received 16 June 2019

Received in revised form

4 September 2019

Accepted 24 September 2019

Available online xxx

#### Keywords:

Enzymatic electrodes

Renewable energy

### ABSTRACT

Enzymatic biofuel cells are a subclass of biofuel cells, which employ enzymes to generate energy from renewable sources. In this study, 3-dimensional graphene (3DG)/glucose oxidase (GOx) bio-nanocomposite was fabricated in order to improve enzyme immobilisation and enzyme lifetime with an enhanced electron transfer rate. These enhancements are due to the unique physical properties of 3DG, e.g. high porosity, large surface area, and excellent electrical conductivity. A power density of 164  $\mu\text{W cm}^{-2}$  at 0.4 V was achieved from this enzymatic biofuel cell (EBFC) with an acceptable performance compared to that of the other glucose biofuel cells (GBFCs). The 3DG enhances the enzyme lifetime, decreases enzyme leaking and, due to its good conductivity, facilitates the electron harvest and transfer from the enzyme active site to the electrode. This suggests that 3DG could be

\* Corresponding author.

E-mail addresses: [arman\\_i06@yahoo.com](mailto:arman_i06@yahoo.com), [arman\\_amani@um.edu.my](mailto:arman_amani@um.edu.my) (A.A. Babadi).

<https://doi.org/10.1016/j.ijhydene.2019.09.185>

0360-3199/© 2019 Hydrogen Energy Publications LLC. Published by Elsevier Ltd. All rights reserved.

Bio-electrocatalysis  
Bioanodes  
3D graphene

used as effective support for enzyme immobilisation on the surface of the electrode in EBFC applications and related areas such as biosensors, bioreactors and implantable bio-fuel cells.

© 2019 Hydrogen Energy Publications LLC. Published by Elsevier Ltd. All rights reserved.

## Introduction

Biofuel cells are a favourable next-generation green energy alternative [1]. Enzymatic biofuel cells, a subclass of biofuel cells, utilise enzymes to generate electricity from renewable fuels such as carbohydrates, urea and organic acids through electrochemical oxidation occurring at the anode [2,3]. They are unique compared to other conventional energy systems because they are cost-effective, generate electricity from renewable sources, enable enzyme selectivity towards the fuel and can be utilised in physiological pH and temperature [4], though they have smaller power density and energy density [5,6]. These benefits make them a suitable choice for powering up implantable medical devices such as pacemakers and micro-drug pumps, and they are even used in wastewater treatment [7–9], drug delivery [10], biosensors [11], remote sensing and communication devices in bioelectronics [12,13]. Glucose oxidase (GOx) is the most preferred enzyme in enzymatic biofuel cells (EBFCs), due to the availability and high selectivity towards glucose [14].

Biofuel cells utilise the abundance of glucose or other carbohydrates present in animal fluids. The most challenging part in cell fabrication is the efficient immobilisation of the enzyme on the electrode surface [15,16]. The limitations of GOx immobilisation on the electrode surface include the enzyme leaching, shorter enzyme lifetime and the poor electron transfer between the enzyme active site and the electrode, which accounts for the lower energy density and power density [17,18].

Based on our knowledge, several methods have been developed to increase the biological function, stability and efficacy of GOx immobilisation on the electrode surface. The entrapment or covalent immobilisation of GOx in stable matrixes such as nanostructured and mesostructured metal oxides [19,20], metal nanoparticles [21,22], conducting polymers [23–25], mesostructured silica [26], sol-gel matrixes [27,28], carbon nanotubes [29,30], graphene [31–33], etc. leads to a faster electron transfer rate and improved enzyme stability [34]. The enzymes' immobilisation platforms prepared from nanostructured composite and hybrid materials such as nanoparticles, nanofibers and nanocarbons are the focus of intense fundamental and applied research [35]. Graphene, a carbon polymorph, is a critical material which immobilises the enzyme and enhances the electrical conductivity between the enzyme active site and the electrode surface [36].

Graphene possesses extraordinary physicochemical properties such as a highly specific surface area [37,38] and an easily modified surface area [39,40], in addition to excellent mechanical, thermal and chemical stability [41] and excellent electronic properties. Thus, graphene is increasingly used in

various applications such as catalysis, sensors, environmental remediation, and energy storage and conversion.

The large surface area of graphene-based nanomaterials and the excellent electrical conductivity create ideal immobilisation support for biomolecules such as enzymes [42–46]. Numerous studies on the direct electron transfer (DET) behaviour of GOx on graphene decorated glassy carbon electrode (GCE) are also reported [47–51]. In recent years, there have been several reports on graphene-based modified electrodes for biofuel cell applications [52,53]. Despite various applications of EBFCs, some drawbacks persist such as enzyme leakage and low power density due to the sluggish electron transfer between the enzyme and the electrode surface, which is the principal research focus in EBFCs [54]. In order to overcome these drawbacks, a GCE/3DG-GOx bio-nanohybrid was prepared and utilised as the bioanode in EBFCs. The results in this work were encouraging, as the 3DG biocatalyst support enhanced the electrical conductivity between the GOx enzyme and the GCE.

## Experimental methodology

### Chemicals

Graphite powder (<45  $\mu\text{m}$ ;  $\geq 99.99\%$ ),  $\text{H}_2\text{SO}_4$  (0.5 M),  $\text{H}_3\text{PO}_4$  (85%),  $\text{KMnO}_4$  (97%),  $\text{Na}_2\text{HPO}_4$ ,  $\text{NaH}_2\text{PO}_4$ , KCl and GOx (type vii from *Aspergillus niger*) were procured from Sigma-Aldrich (Dorset, UK). The supporting electrolyte in the electrochemical experiments was 0.1M of phosphate buffer solution (pH 7), prepared by dissolving equimolar  $\text{Na}_2\text{HPO}_4$  and  $\text{NaH}_2\text{PO}_4$  with KCl in deionised water.

### Instrumentation

All electrochemical experiments were performed using a computer-controlled 302N Autolab potentiostat/galvanostat (Ecochemie, Netherlands) with a conventional three-electrode system in a 50 ml cell. The modified glassy carbon electrode (GCE, diameter 3 mm) was the working electrode, while a thin Pt wire and Ag/AgCl (3M KCl) were the counter and reference electrodes, respectively. The Raman spectra of the 3D-graphene composite were obtained using a Renishaw inVia™ (M005-141) confocal Raman microscope employing a 532 nm excitation wavelength to confirm the reduction of graphene. The Fourier transform infrared (FTIR) spectroscopy of samples was characterised by a Bruker IFS 66/S FTIR with a  $4\text{ cm}^{-1}$  resolution. The resolution of the FTIR was set to  $4\text{ cm}^{-1}$ , with 16 scans in the wavelength range of  $400\text{--}4000\text{ cm}^{-1}$ .

## Preparation of bioanode

### Preparation of 3DG

The initial step for the development of 3DG is the synthesis of graphitic oxide from graphite flakes using the modified Hummer's method [55,56]. Graphene oxide (GO) was obtained through the oxidation of 1 g of graphite flakes with 120 ml of  $\text{H}_2\text{SO}_4$ , 13 ml of  $\text{H}_3\text{PO}_4$  and 6 g of  $\text{KMnO}_4$ . The mixture was stirred for 3 days to complete the oxidation of graphite. During oxidation, the colour of the mixture changed from dark purple-green to dark brown. To stop the oxidation process, about 150 g of ice cube was added into the reaction, followed by 7 ml of  $\text{H}_2\text{O}_2$  solution, with the colour of the mixture changing to bright yellow due to the severe oxidation of graphite. The graphitic oxide was washed three times with 1 M of HCl with centrifugation and repeatedly washed with deionised water until the pH reached 4–5. During the washing process with deionised water, the graphitic oxide was exfoliated, resulting in the thickening of the GO solution due to the formation of GO gel.

A mixture of 1 ml GO aqueous dispersion, and 40 ml of deionised water was stirred for 20 min to prepare a homogeneous solution. Then, 10  $\mu\text{l}$  of hydrazine was added into the mixture with stirring, and the pH was adjusted to 9. The dispersion was sealed in a 50 ml stainless steel autoclave and maintained at 80 °C for 24 h. The prepared 3DG was removed with tweezers and kept in a freeze drier for 48 h in order to remove absorbed water. The dried 3DG was stored in a sealed Schott bottle for the next step.

### Fabrication of 3DG modified glassy carbon electrode (GCE)

The synthesised 3DG (10 mg) was placed in a test tube containing 5 ml of ethanol, ultrasonicated for 30 min to provide a homogeneous dispersion and left to cool to room temperature for 10 min. In the following step, 5 mg of glucose oxidase (GOx) enzyme was added into the solution and mixed gently before being stored in a fridge.

The GCE (3 mm diameter) was polished with 0.05 mm of alumina slurry on a velvet pad. Before the modification, the GCE was placed in a beaker containing 1:1 v/v double distilled water and ethanol. Then the GCE was ultrasonicated for 5 min, washed with deionised water and left to dry at room temperature ( $25 \pm 3$  °C). After drying, 5  $\mu\text{L}$  of the prepared 3DG-GOx dispersion was drop-casted onto the GCE surface and left to dry at room temperature ( $25 \pm 3$  °C) for 15 min.

## Results and discussions

### Spectroscopic studies

Raman spectroscopy is a powerful tool to characterise the presence of disorder in carbon nanostructures. Fig. 1(A) shows the comparison between the Raman spectra of GO and 3DG.

As can be seen in Fig. 1(A), the spectra of all samples show two peaks at around  $1584\text{ cm}^{-1}$  and  $1351\text{ cm}^{-1}$ , related to the G and D bands of RGO, respectively. The G band is assigned to the first-order scattering of the  $\text{E}_{2g}$  phonon, while the D band is attributed to the decreasing size of the  $\text{sp}^2$  domains due to the

extensive oxidation on the GO nanosheets [57]. The ratio between the D and G band intensity ( $I_D/I_G$ ) represents the amount of disorder, which is expressed by the ratio of  $\text{sp}^2/\text{sp}^3$  carbon, which increases (from 1.184 to 1.386) after the reduction of GO. Compared to GO (0.93), the 3DG (1.01) has a slightly higher  $I_D/I_G$  ratio, which is attributed to the decrease in the size of the  $\text{sp}^2$  domains after the reduction process.

The comparison of the FTIR spectrum between GO and 3DG is presented in Fig. 1(B). The peak in the FTIR spectrum of GO at  $1158\text{ cm}^{-1}$  is attributed to the C–O and C–OH group stretching vibration, while the peak at  $1741\text{ cm}^{-1}$  is assigned to the carbonyl C=O stretch, and the broad wave between  $2500\text{ cm}^{-1}$  and  $3500\text{ cm}^{-1}$  is due to the hydroxyl O–H stretch from the OH groups and the presence of moisture in the GO [58]. The absence of the peaks attributed to the C=O, C–O and O–H groups in the FTIR spectrum of 3DG confirms the successful synthesis of 3DG and the reduction of GO.

### Morphology characterisation of 3DG

The two factors which control the power density and long-term activity of biofuel cells are the enzyme stability and the diffusion towards the electrode surface. The microporous structure of 3DG can prevent the denaturation of the immobilised enzyme, enzyme leaching, and provide a sufficient concentration of both glucose and oxygen to the enzymes. The morphology of the bioanode was characterised by field emission scanning electron microscopy (FESEM) and high-resolution transmission electron microscopy (HRTEM). Fig. 2(A) shows the HRTEM image of the synthesised 3DG, while the FESEM image (Fig. 2B) reveals a highly porous structure of the 3DG, which improves the biological function, stability and efficacy of GOx immobilisation. As it is apparent in Fig. 2(C), the GOx enzyme has been trapped inside the porous structure of 3DG through the physical absorption, and we have a successful hybridisation of 3DG/GOx. This is the simplest method of immobilisation which developed base on the hydrogen bonds and Van der Waal's forces. It is based on the physical interaction of enzyme and 3-dimensional graphene. Also, due to not employing any reagent comparing to chemical methods, it is less disruptive to the enzyme protein structure. Furthermore, physical adsorption is cheap, easy to carry out, and minimum steps of activation required [59].

### Electrochemical performances of bioanode

The immobilisation of GOx on the GCE/3DG was confirmed by cyclic voltammetry (CV) (five cycles repeated). Line (a), in Fig. 3(A) presents the CV of the GCE/3DG-GOx at pH 7, which shows a pair of redox peaks (oxidation and reduction reactions) at  $-0.43\text{ V}$  and  $-0.39\text{ V}$ .

In contrast, the CV of GCE/GOx (line b) does not show any electrochemical peaks. These results suggest that the fabricated 3DG-GOx bio-nanocomposite enhances the electron transfer process between the electrode surface and the enzyme.

The effect of different scan rates on the GCE/3DG-GOx was also studied by varying the scan rates from  $1\text{ mVs}^{-1}$  to  $100\text{ mVs}^{-1}$  in nitrogen saturated solution at pH 7. According to

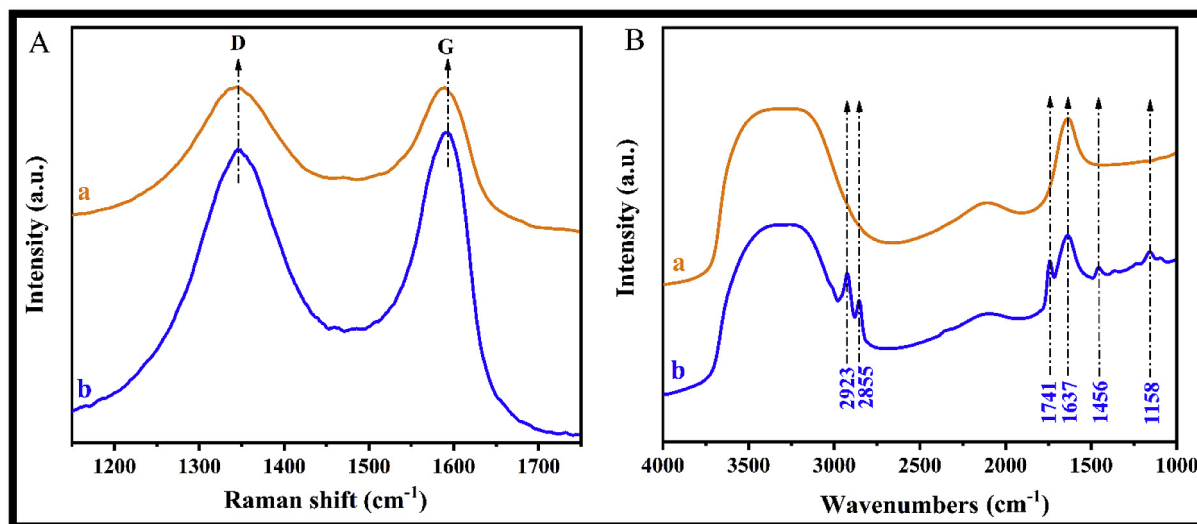


Fig. 1 – (A) Raman spectra, and (B) FTIR spectrum of a: GO and b: 3DG.

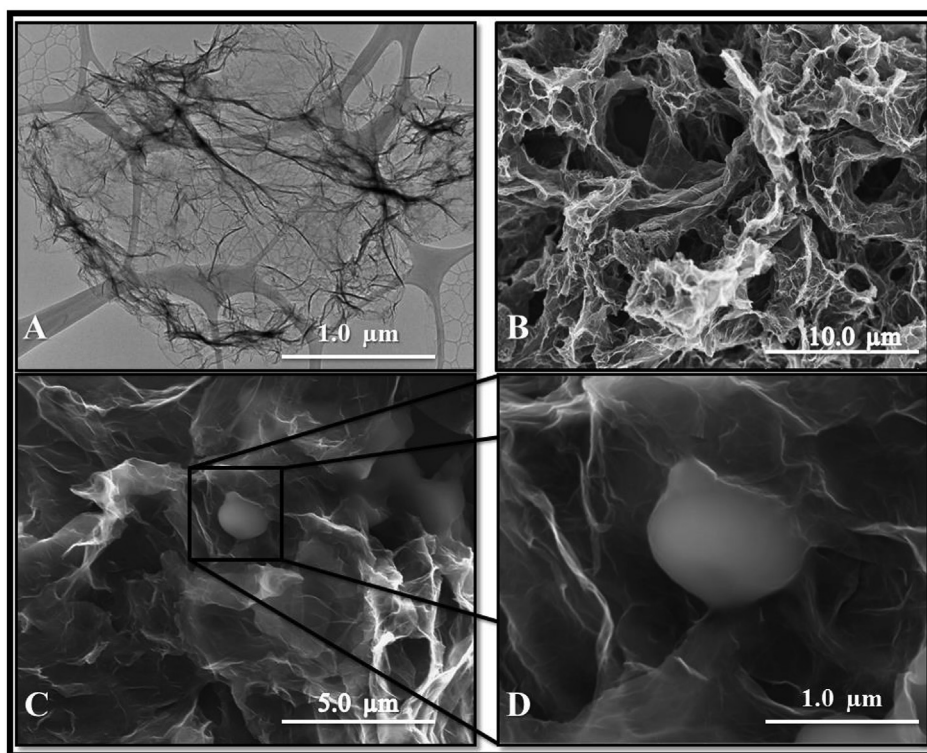
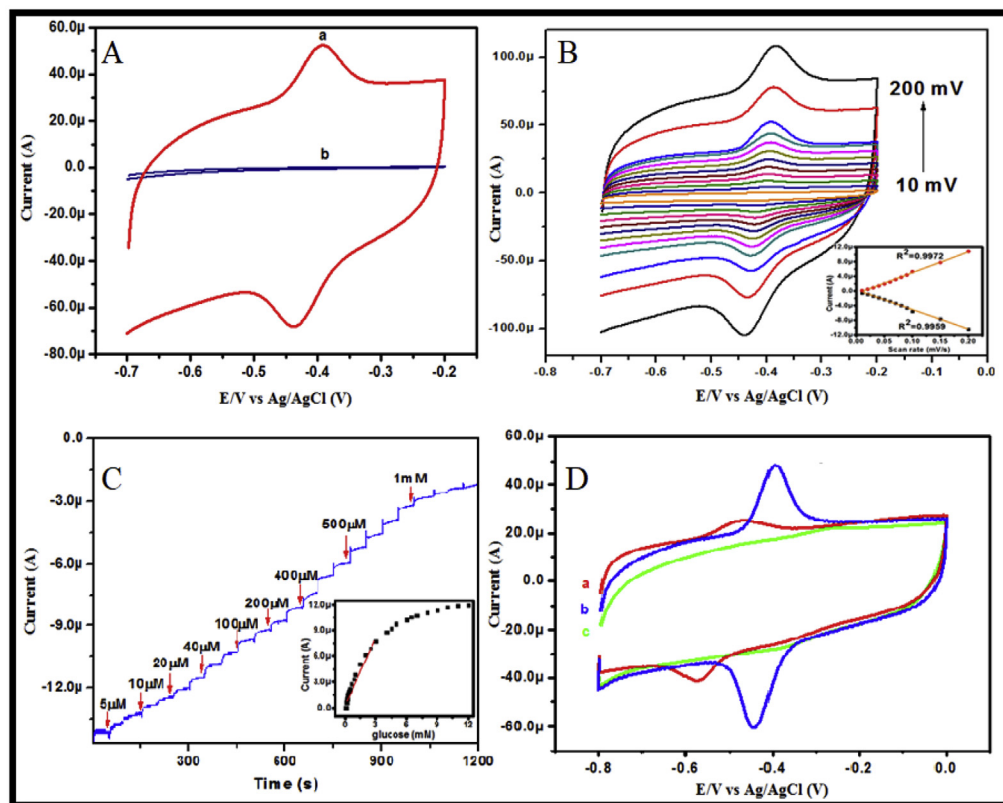


Fig. 2 – (A) HRTEM image of 3DG, (B) FESEM image of 3DG, (C) The hybrid of GOx and 3DG and (D) immobilised GOx on 3DG.

Fig. 3(B), the peak current is linearly dependent on the scan rate, while the peak potential is shifted towards the negative region with the increase of the scan rate from 10 to 200 mVs<sup>-1</sup>. These results confirm that the electron transfer is a quasi-reversible process, while the diffusion is controlled through a surface diffusion process and not through solution diffusion. It means that the electron transfer rate between the working electrode and the species in the solution is fast, but still, there are some thermodynamic barriers. This suggests that the

electron transfer between the GOx enzyme and the electrode surface is a quasi-reversible process, wherein the GOx retains its bioactivity even at high scan rates. Fig. 3(C) presents the chronoamperometric response of the GCE/3DG-GOx bio-nanocomposite based on the current-time plot for successive additions of glucose at -0.40 V in an O<sub>2</sub> saturated 0.1 M PBS (pH 7) solution. From Fig. 3(C), the current increases with the addition of glucose and reaches a steady-state within 5 s. The amperometric current increases linearly with the



**Fig. 3** – (A) CV of the GCE/3DG-GOx at pH 7; (a) bare GCE, (b) GCE/3DG-GOx, (B) GCE/3DG-GOx at different scan rates in  $N_2$  saturated solution at pH 7. The scan rates from inner to outer are: 10, 20, 30, 40, 50, 60, 70, 80, 90, 100, 150, 200  $mV s^{-1}$ . Inset is the linear dependence of  $I_{pa}$  (■), and  $I_{pc}$  (■) on the scan rate (10–200  $mV s^{-1}$ ), (C) Chronoamperometric response of the GCE/3DG-GOx to successive injection of glucose into air saturated 0.1 M PBS (pH 7.0) at  $-0.40 V$ , (D) The CV of GCE/3DG-GOx at 100  $mV s^{-1}$  in buffer solutions at different pH values; (a) pH 10, (b) pH 7 and (c) pH 4.

concentration of glucose from 0.05 to 3 mM. Considering that the average blood glucose level is between 4 and 6 mM, the EBFC could be supplied with a sufficient amount of glucose for implant applications. The CV of GCE/3DG-GOx at 100  $mV s^{-1}$  in buffer solutions with a different pH is shown in Fig. 3(D). The CV shows a negative shift of the redox peaks with increasing pH values from 4 to 10 at 100  $mV s^{-1}$ .

Electrochemical impedance spectroscopy (EIS) of the modified electrodes was performed in order to investigate the effect of enzyme catalysts on the charge transfer process of the EBFC bioanodes. The charge transfer resistance ( $R_{ct}$ ) of each bioanode was obtained from the Nyquist plot. Fig. 4(A) shows the Nyquist plots ( $-Z''$  vs.  $Z'$ ) of the enzyme immobilised 3DG modified GCE, the GCE/3DG and the GCE/GOx. From the Nyquist plots, the GCE/GOx has the highest  $R_{ct}$  value, followed by the GCE/3DG/GOx. The lowest  $R_{ct}$  value was reported for the 3DG modified GCE. These results show the significant role of 3DG in enhancing the electron transfer between the enzyme active site and surface of the GC electrode and decreasing the electrical resistance. The bioanodes show different values of  $R_{ct}$  obtained from the Nyquist plots. GOx is a protein molecule with negligible electronic conductivity. Thus, the  $R_{ct}$  increases with the loading amount of the GOx enzyme. It should be noted that the intercepts on the real axis in the Nyquist plots are similar for all bioanodes. This

demonstrates that the solution resistance ( $R_s$ ) of the bioanodes is unaffected by the types of biocatalysts.

Tafel polarization measurements were also performed in order to evaluate the performance of the fabricated bioanodes. The observed open circuit potential (OCP) of 0.44 V is much less than the reported OCPs for 3DG aggregated electrodes with DET. As mentioned previously, the fabricated GBFC is polarised by connecting the fabricated electrode to a range of the resistors. Fig. 4(B) represents the potential and power density of the cell as a function of current. This indicates that the 3DG/GOx modified GCE can supply a power density of approximately 160  $\mu W cm^{-2}$  at 0.4 V. The higher power density observed in this work compared to previous reports indicates the critical role of 3DG in the enhancement of enzyme immobilisation and the increased electron transfer process, with both factors being crucial for improved performance of the EBFC.

In order to evaluate the stability of the 3DG/GOx modified GCE, the bioanode stored in PBS buffer (pH 7) at 4 °C and tested every day. After the first day of fabrication, it had lost 13% of its original power output. It was found out that the power output decays slowly and become 60% of the initial power density after 7 days, as illustrated in Fig. 4(C).

Table 1 present a power generation comparison between the reported carbon-based EBFCs in previous studies and the

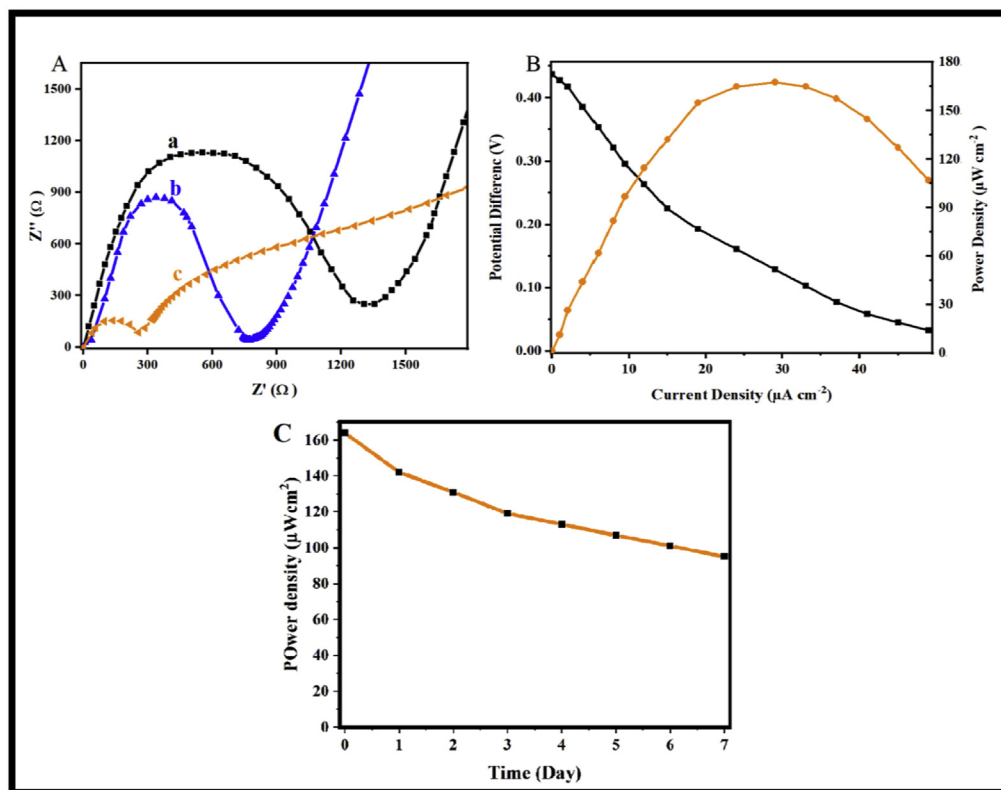


Fig. 4 – (A) Nyquist plots in 0.1 M PBS (pH 7), (a) bare GCE; (b) 3DG modified GCE; (c) 3DG/GOx modified GCE, (B) Polarization curve of the fabricated 3DG/GOx modified GCE in 0.1 M PBS (pH 7), (C) The operation stability of fabricated bioanode as a function of time.

3DG/GOx modified GCE, which have been fabricated in this study. According to this table, the power density of fabricated bioanode is among top three reported biofuels cells. The performance merit of the GCE/3DG-GOx bioanode places it right after the PABMSA modified BP and vaCNTs, but before the graphene–AuNP hybrid. This is a noticeable power density

while the fabrication process of 3DG/GOx modified GCE is much easier, and no functionalization is required comparing to other competitors.

## Conclusions

A 3DG modified bioanode was fabricated in this study in order to enhance the performance of the EBFCs, i.e. to increase the lifetime of the enzyme, overcome the enzyme leaching and improve the electrode transfer between the enzyme active site and the electrode surface. In this study, we synthesised a highly porous, conductive 3DG and utilised it as an electrode platform for the immobilisation of the GOx enzyme. The fabricated bioanode in this study has a maximum power density of  $164 \mu\text{Wcm}^{-2}$  at a cell voltage of 0.4 V.

In conclusion, the highly porous structure of 3DG entraps the GOx enzyme and decreases enzyme leaching, thus increasing the enzyme lifetime by maintaining the 3D structure. The excellent electrical conductivity of 3DG facilitates the DET between the active site of the GOx and the modified GCE and decrease the resistance toward the electron flow. The results demonstrated the high performance of the fabricated GCE/3DG-GOx as a bioanode for EBFC applications. The synthesised 3DG is a versatile electrode platform for the immobilisation of other enzymes in the construction of EBFCs and third-generation enzymatic biosensors.

Table 1 – Carbon based EBFCs power generation comparison.

Material	Enzyme	Power density ( $\mu\text{W cm}^{-2}$ )	Ref.
Gold/MWCNT	GOx	42	[60]
NH <sub>2</sub> -CNTs	GDH	45	[61]
PABMSA via BP & vaCNTs	GDH	122	[62]
Graphene–AuNP hybrid	GOx	196	[63]
PEDOT-coated MWCNT	GOx	640	[64]
3D Graphene	GOx	164	Present study

MWCNT: Multiwall Carbon Nanotubes.

NH<sub>2</sub>: amino group.

CNTs: Carbon Nanotubes.

PABMSA: Poly (3-aminobenzoic acid-co-2-methoxyaniline-5-sulfonic acid).

vaCNTs: Vertically Aligned Carbon Nanotubes.

PEDOT: Poly(3,4-Ethylenedioxythiophene).

## Acknowledgements

We are grateful to the University of Malaya for funding awarded to Dr. Wan-Mohtar under Fundamental Research Grant Scheme (FRGS: FP066-2018A), Research University Grant (RU300I-2017) and to Dr. Zul Ilham under Faculty Research Grant (GPF016B-2018) and SATU Joint Research Grant (SATU ST006-2019).

## REFERENCES

- [1] Devadas B, Mani V, Chen S-M. A glucose/O<sub>2</sub> biofuel cell based on graphene and multiwalled carbon nanotube composite modified electrode. *Int J Electrochem Sci* 2012;7(9):8064–75.
- [2] Babadi AA, Bagheri S, Hamid SBee A. Progress on implantable biofuel cell: nano-carbon functionalization for enzyme immobilization enhancement. *Biosens Bioelectron* 2016;79:850–60.
- [3] Ahmad A, et al. Use of enzymes in different types of biofuel cells, vol. 44; 2019. p. 29.
- [4] Zebda A, et al. Membraneless microchannel glucose biofuel cell with improved electrical performances. *Sens Actuators B Chem* 2010;149(1):44–50.
- [5] Topcagic S, Minter SD. Development of a membraneless ethanol/oxygen biofuel cell. *Electrochim Acta* 2006;51(11):2168–72.
- [6] Lin J, et al. Bio-fuel reformation for solid oxide fuel cell applications. Part 1: fuel vaporization and reactant mixing. *Int J Hydrogen Energy* 2013;38(27):12024–34.
- [7] Gao F, et al. An enzymatic glucose/O<sub>2</sub> biofuel cell: preparation, characterization and performance in serum. *Electrochem Commun* 2007;9(5):989–96.
- [8] Barton SC, Gallaway J, Atanassov P. Enzymatic biofuel cells for implantable and microscale devices. *Chem Rev* 2004;104(10):4867–86.
- [9] Sun J, et al. Improved performance of air-cathode single-chamber microbial fuel cell for wastewater treatment using microfiltration membranes and multiple sludge inoculation. *J Power Sources* 2009;187(2):471–9.
- [10] Zhou M, et al. A self-powered "sense-act-treat" system that is based on a biofuel cell and controlled by boolean logic. *Angew Chem Int Ed Engl* 2012;51(11):2686–9.
- [11] Zhou M, et al. DNAzyme logic-controlled biofuel cells for self-powered biosensors. *Chem Commun* 2012;48(32):3815–7.
- [12] El Ichi-Ribault S, et al. Remote wireless control of an enzymatic biofuel cell implanted in a rabbit for 2 months, vol. 269; 2018. p. 360–6.
- [13] Chen T, et al. A miniature biofuel cell. *J Am Chem Soc* 2001;123(35):8630–1.
- [14] Unnikrishnan B, Palanisamy S, Chen S-M. A simple electrochemical approach to fabricate a glucose biosensor based on graphene–glucose oxidase biocomposite. *Biosens Bioelectron* 2013;39(1):70–5.
- [15] Liu C, et al. Membraneless enzymatic biofuel cells based on graphene nanosheets. *Biosens Bioelectron* 2010;25(7):1829–33.
- [16] Rodríguez-Padrón D, et al. Highly efficient direct oxygen electro-reduction by partially unfolded laccases immobilized on waste-derived magnetically separable nanoparticles. *Nanoscale* 2018;10(8):3961–8.
- [17] House JL, Anderson EM, Ward WK. Immobilization techniques to avoid enzyme loss from oxidase-based biosensors: a one-year study. *Journal of Diabetes Science and Technology (Online)* 2007;1(1):18–27.
- [18] Yang X, et al. Covalent immobilization of an enzyme (glucose oxidase) onto a carbon sol–gel silicate composite surface as a biosensing platform. *Anal Chim Acta* 2003;478(1):67–75.
- [19] Cao H, et al. A glucose biosensor based on immobilization of glucose oxidase into 3D macroporous TiO<sub>2</sub>. *Electroanalysis* 2008;20(20):2223–8.
- [20] Fang B, et al. A glucose oxidase immobilization platform for glucose biosensor using ZnO hollow nanospheres. *Sens Actuators B Chem* 2011;155(1):304–10.
- [21] Bharathi S, Nogami M. A glucose biosensor based on electrodeposited biocomposites of gold nanoparticles and glucose oxidase enzyme. *Analyst* 2001;126(11):1919–22.
- [22] Baby TT, et al. Metal decorated graphene nanosheets as immobilization matrix for amperometric glucose biosensor. *Sens Actuators B Chem* 2010;145(1):71–7.
- [23] Ekiz F, et al. Electrochemical Polymerization of (2-Dodecyl-4,7-di (thiophen-2-yl)-2H-benzo[d][1,2,3] triazole): a Novel Matrix for Biomolecule Immobilization. *Macromol Biosci* 2010;10(12):1557–65.
- [24] Back matter. *J Chem Soc, Faraday Trans 1: Physical Chemistry in Condensed Phases* 1986;82(5):P055–66.
- [25] Alwarappan S, et al. Enzyme-doped graphene nanosheets for enhanced glucose biosensing. *J Phys Chem C* 2010;114(30):12920–4.
- [26] Blin JL, et al. Direct one-step immobilization of glucose oxidase in well-ordered mesostructured silica using a nonionic fluorinated surfactant. *Chem Mater* 2005;17(6):1479–86.
- [27] Jia W-Z, et al. One-step immobilization of glucose oxidase in a silica matrix on a Pt electrode by an electrochemically induced sol-gel process. *Langmuir* 2007;23(23):11896–900.
- [28] Chen Q, Kenausis GL, Heller A. Stability of oxidases immobilized in silica gels. *J Am Chem Soc* 1998;120(19):4582–5.
- [29] Lin Y, et al. Glucose biosensors based on carbon nanotube nanoelectrode ensembles. *Nano Lett* 2004;4(2):191–5.
- [30] Periasamy AP, Chang Y-J, Chen S-M. Amperometric glucose sensor based on glucose oxidase immobilized on gelatin-multiwalled carbon nanotube modified glassy carbon electrode. *Bioelectrochemistry* 2011;80(2):114–20.
- [31] Shan C, et al. Direct electrochemistry of glucose oxidase and biosensing for glucose based on graphene. *Anal Chem* 2009;81(6):2378–82.
- [32] Kang X, et al. Glucose oxidase–graphene–chitosan modified electrode for direct electrochemistry and glucose sensing. *Biosens Bioelectron* 2009;25(4):901–5.
- [33] Zhou K, et al. Electrocatalytic oxidation of glucose by the glucose oxidase immobilized in graphene-Au-nafion biocomposite. *Electroanalysis* 2010;22(3):259–64.
- [34] Joshi RK, et al. Graphene films and ribbons for sensing of O<sub>2</sub>, and 100 ppm of CO and NO<sub>2</sub> in practical conditions. *J Phys Chem C* 2010;114(14):6610–3.
- [35] Misson M, Zhang H, Jin B. Nanobiocatalyst advancements and bioprocessing applications. *J R Soc Interface* 2015;12(102). 20140891.
- [36] Putzbach W, Ronkainen NJ. Immobilization techniques in the fabrication of nanomaterial-based electrochemical biosensors: a review. *Sensors* 2013;13(4):4811–40.
- [37] Xie T, et al. A unique carbon with a high specific surface area produced by the carbonization of agar in the presence of graphene. *Chem Commun* 2013;49(88):10427–9.
- [38] Babadi, A.A., S. Bagheri, and S.B.A. Hamid, Progress ON antimicrobial surgical gloves: a review. *Rubber Chemistry and Technology*. 0(0): p. null.
- [39] Sur UK. Graphene: a rising star on the horizon of materials science. *Int J Electrochem* 2012;2012:12.

- [40] Ramimoghdam D, Bagheri S, Abd hamid SB. Biotemplated Synthesis of anatase titanium dioxide Nanoparticles via lignocellulosic waste material. *BioMed Res Int* 2014;2014:7.
- [41] Lee W, et al. Simultaneous enhancement of mechanical, electrical and thermal properties of graphene oxide paper by embedding dopamine. *Carbon* 2013;65(0):296–304.
- [42] Ge J, et al. Nanobiocatalysis in organic media: opportunities for enzymes in nanostructures. *Top Catal* 2012;55(16–18):1070–80.
- [43] Jin L, et al. Functionalized graphene oxide in enzyme engineering: a selective modulator for enzyme activity and thermostability. *ACS Nano* 2012;6(6):4864–75.
- [44] Pavlidis IV, et al. Development of effective nanobiocatalytic systems through the immobilization of hydrolases on functionalized carbon-based nanomaterials. *Bioresour Technol* 2012;115(0):164–71.
- [45] Gokhale AA, Lu J, Lee I. Immobilization of cellulase on magnetoresponsive graphene nano-supports. *J Mol Catal B Enzym* 2013;90(0):76–86.
- [46] Chekin F, et al. Preparation and characterization of Ni(II)/polyacrylonitrile and carbon nanotube composite modified electrode and application for carbohydrates electrocatalytic oxidation. *J Solid State Electrochem* 2012;16(10):3245–51.
- [47] Jiang B, et al. Hydrophilic immobilized trypsin reactor with magnetic graphene oxide as support for high efficient proteome digestion. *J Chromatogr A* 2012;1254(0):8–13.
- [48] Pavlidis I, et al. Regulation of catalytic behaviour of hydrolases through interactions with functionalized carbon-based nanomaterials. *J Nanoparticle Res* 2012;14(5):1–10.
- [49] Shao Q, et al. Insight into the effects of graphene oxide sheets on the conformation and activity of glucose oxidase: towards developing a nanomaterial-based protein conformation assay. *Phys Chem Chem Phys* 2012;14(25):9076–85.
- [50] Zhang Y, et al. Assembly of graphene oxide–enzyme conjugates through hydrophobic interaction. *Small* 2012;8(1):154–9.
- [51] Kane RS, Stroock AD. Nanobiotechnology: protein-nanomaterial interactions. *Biotechnol Prog* 2007;23(2):316–9.
- [52] Zheng W, et al. A glucose/O<sub>2</sub> biofuel cell base on nanographene platelet-modified electrodes. *Electrochem Commun* 2010;12(7):869–71.
- [53] Gonzalez-Solino C, Lorenzo MJB. Enzymatic fuel cells: towards self-powered implantable and wearable diagnostics. *Biosensors* 2018;8(1):11.
- [54] Osman M, et al. Recent progress and continuing challenges in bio-fuel cells. Part I: enzymatic cells. *Biosensors and Bioelectronic* 2011;26(7):3087–102.
- [55] Guo H-L, et al. A green approach to the synthesis of graphene nanosheets. *ACS Nano* 2009;3(9):2653–9.
- [56] Hummers Jr WS, Offeman RE. Preparation of graphitic oxide. *J Am Chem Soc* 1958;80(6). 1339-1339.
- [57] Reich S, Thomsen C. Raman spectroscopy of graphite. *Philos Trans R Soc London, Ser A: Mathematical, Physical and Engineering Sciences* 2004;362(1824):2271–88.
- [58] Liu ST, et al. Bio-cathode materials evaluation and configuration optimization for power output of vertical subsurface flow constructed wetland - microbial fuel cell systems. *Bioresour Technol* 2014;166:575–83.
- [59] Kragl U, Greiner a, Wandrey C. Enzymes, immobilized, reactors. In: *Encyclopedia of bioprocess technology*; 2002.
- [60] Campbell AS, et al. Improved power density of an enzymatic biofuel cell with fibrous supports of high curvature. *RSC Adv* 2016;6(12):10150–8.
- [61] Korani A, Salimi A. High performance glucose/O<sub>2</sub> compartment-less biofuel cell using DNA/CNTs as platform for immobilizing bilirubin oxidase as novel biocathode and integrated NH<sub>2</sub>-CNTs/dendrimer/glucose dehydrogenase/nile blue as bioanode. *Electrochim Acta* 2015;185:90–100.
- [62] Göbel G, et al. Application of modified carbon nanotube materials for enzymatic biofuels cells based on direct enzyme-electrode contacts. *Meet Abstr* 2015;(32):1198. MA2015–02.
- [63] Chen Y, et al. Design of an enzymatic biofuel cell with large power output. *J Mater Chem* 2015;3(21):11511–6.
- [64] Kwon CH, et al. Stability of carbon nanotube yarn biofuel cell in human body fluid. *J Power Sources* 2015;286:103–8.